Malaysian Journal of Chemistry, 2024, Vol. 26(5), 194-208
(Special Issue: *3rd Virtual International Symposium on Sciences 2023*)

Molecular Docking Studies of Phytochemicals from *Azadirachta indica* with Trehalose–6-Phosphate Phosphatase of Pathogenic Microbes

Adam Azmihan[1], Nurul Anis Johari[1], Mohamad Zakkirun Abdullah[2]* and Latifah Munirah Bakar[1]*

[1]School of Biology, Faculty of Applied Sciences, Universiti Teknologi MARA, Shah Alam, 40450 Shah Alam, Selangor, Malaysia

[2]Department of Fundamental Dental and Medical Sciences, Kulliyyah of Dentistry, International Islamic University Malaysia, 25200 Kuantan, Pahang, Malaysia

*Corresponding author (e-mail: zakkirun@iium.edu.my, latifahmunirah@uitm.edu.my)

Trehalose-6-phosphate phosphatase (TPPs) is a particular enzyme involved in the biosynthesis pathways of trehalose that are often connected to the virulence of pathogenic microbes. Therefore, TPPs are targeted for therapeutic purposes. The inhibition of its biosynthesis pathway can achieve this. *Azadirachta indica* (*A. indica*), despite its wide use in traditional medicine, received less attention when studying the bioactive compounds for antimicrobial properties. Therefore, this study aims to investigate the potential of phytochemicals from Azadirachta indica as a therapeutic agent against TPPs of pathogenic microbes via in silico analysis. Molecular docking was conducted using 30 selected phytochemicals from *A. indica* against TPPs from *Candida albicans* (PDB: 5DXI), *Cryptococcus neoformans* (PDB: 5DX9), and *Salmonella Typhimurium* (PDB: 6UPD) with ampicillin, fluconazole, and isoniazid acting as control ligand. Molecular docking was performed using AutoDock Vina. The molecular docking analysis indicates that phytochemicals from *A. indica* contain the potential to generate a high binding affinity with the TPPs. The highest binding affinity generated by *A. indica*'s phytochemicals against TPPs from *Candida albicans* (PDB: 5DXI), *Cryptococcus neoformans* (PDB: 5DX9), and *Salmonella Typhimurium* (PDB: 6UPD) is catechin (-9.0 kcal/mol), margocin (-9.9 kcal/mol) and catechin (-9.0 kcal/mol), respectively. Concisely, the phytochemicals of *A. indica* showed a promising potential to act as an inhibitor of trehalose biosynthesis pathways, subsequently to be applied as alternative therapeutic approaches for antibiotic purposes.

Keywords: Molecular docking; *Azadiracta indica*; in silico; phytochemicals; trehalose-6-phosphate-phosphatase

Received: November 2023; Accepted: February 2024

Trehalose is an essential sugar considered an important stress protectant against abiotic stresses such as heat, nutritional deficit, high osmolarity, oxidation, and UV-B irradiation. Studies have shown that the trehalose biosynthesis pathways involving the enzyme trehalose-6-phosphate-phosphatase (TPPs) play a vital role in virulence and pathogenesis, especially those of fungi and bacteria [1, 2]. These pathways also involve other cell activities, such as susceptibility to oxidative stress, cell wall integrity, mating, capsule production, and sporulation. One of the core enzymes of the most common enzyme trehalose biosynthesis pathways, TPPs, is an attractive target enzyme. TPPs are desirable targets for enzyme inhibition because their accumulation in pathogenic organisms will increase the pathogen's toxicity. This is why biosynthesis pathways for trehalose generate much attention for its therapeutic intervention to combat infectious diseases transmitted from bacteria, helminths, or fungi [3].

In recent years, the looming threat of rising antibiotic resistance within pathogens and the need for suitable cautionary measures has been identified. Even though antibiotic chemotherapeutics are quite effective in treating infectious diseases, antimicrobial resistance among pathogens has proven to be an ever-increasing hurdle against antibiotics [2], highlighting the need for alternative approaches to combat infectious diseases.

Antibiotic resistance within pathogens increases the cost of basic healthcare due to the need for longer and more complicated therapy to treat common infectious diseases. This resistance makes complex medical procedures riskier, leading to additional health complications and higher costs for patients and healthcare systems. Thus, there is an urgency to develop alternative therapies and explore new opportunities that might lead to the discovery of new antibiotics. Scientific advances of past decades enable protein-based drug discovery strategies where the structures and proteins related to pathogen survival can be manipulated in our favor. One of the favored approaches is the selection of pathogen proteins that operate

†Paper presented at the 3rd Virtual International Symposium on Sciences (3rd VISoS 2023)

within the biochemical pathways [4]. This approach can disrupt their ability to survive and replicate, offering a promising strategy for combating antibiotic resistance.

Previously, plants have been in many traditions and cultures and serve as a medicine that has contributed to human health and well-being. Treatment for diseases like diabetes, malaria, and anemia has long revolved around medicinal plants [5]. However, the potential of plants as sources of drugs is still largely unexplored. Neem plant *A. indica* is one of the various plants containing natural bioactive agents belonging to the Meliacae (Mahogany) family. Phytochemical analysis of *A. indica* indicates the presence of several compounds, including tannins, saponins, cardiac glycosides, alkaloids, steroids, and flavonoids [5]. Nimbidin, nimbin, nimbolide, gedunin, mahmoodin, margolone, and cyclic trisulfide are compounds found in neem that contribute to antibacterial activity. These phytochemicals may show antimicrobial properties towards pathogens. Thus, we are interested in screening the potential phytochemicals as drug molecules against TPPs and observing their performance against the biosynthesis pathways of TPP within pathogens.

Structure-based drug design utilizing phytochemical compounds can decrease the ambiguity involved in the experiment and speed up the process. The silico approach or molecular docking has become a way to develop novel drugs and aid researchers in comprehending the best interactivity between the target protein and ligand (active compound) [6]. This method of approach enables the prediction of how a protein (enzyme) would react with small molecules (ligands) by thoroughly examining the ligand-protein binding pose and its binding affinity [7]. Establishing a virtual ligand-protein interaction model can significantly reduce the time, energy, and cost required for drug development by enabling *streamlined in vitro and in vivo approaches*. This study uses molecular docking to investigate the binding affinity of selected phytochemical compounds to the TPPs protein model. This approach can pave the way for developing new drugs that target TPPs and help combat virulent infections and the spread of pathogens.

EXPERIMENTAL

Software and Program

PyMol and *Discovery Studio Biovia 2021* were used to visualize and modify the receptor and ligand structures. *AutoDock Vina* was the main docking program in this work. The PDBQT file format preparation and the grid box determination were done using *AutoDock Tools* version 1.5.7. Post-docking analysis was done using *PyMol* and *DS Biovia 2021*.

Literature Search

A thorough literature search was conducted to identify the potential bioactive compounds of *A.indica*. The crystal structure of bioactive compounds of *A. indica* was obtained from the RCSB Protein Data Bank. The control used in this molecular docking is ampicillin, fluconazole, and isoniazid [8].

Preparation of Ligand Structures Phytochemicals from *A. indica*

The 3D structure of phytochemicals of *A. indica* was downloaded in the Spatial Data File (.SDF) file format from the PubChem Compound Database (https://pubchem.ncbi.nlm.nih.gov/). The SDF file format was converted into the Protein Data Bank Files (.PDB) format using *Discovery Studio Biovia 2021*. *AutoDock Tools 1.5.7* (ADT) prepared ligand structure with Gasteiger changes and rotatable bonds. Structures in the .PDB file formats were then converted to the Protein Data Bank, Partial Charge & Atom Type (PDBQT) file format using ADT, making it eligible for molecular docking using *AutoDockVina*.

Preparation of Macromolecule Structures of the TPPs Protein

The crystal structure of the TPPs protein (PDB: 5DXI, 5DX9, 6UPD) was downloaded from the Research Collaboratory for Structural Bioinformatics website (http://www.rcsb.org). Protein inhibitors were separated using *Discovery Studio Biovia 2021* and used in the redocking step. ADT software was used to prepare the required files for *AutoDock Vina* by removing water, adding polar hydrogen, computing Gasteiger charges to protein structures, and converting protein structures from the .PDB file format to .PDBQT file format.

Grid Box Determination

The location of the grid box was selected using ADT based on the known original inhibitor's location. Grid coordinates were confirmed after serial redocking steps of the inhibitor to the protein with a root-mean-square deviation (RMSD) value below two ångström (Å), which represented good reproduction of the correct pose of predicted structural conformation as compared to observed structural conformation from actual experiments. [7]. Meanwhile, the grid dimension's determination size is based on each ligand's size.

Molecular Docking

Molecular docking was performed using the *AutoDock Vina* [9] program. The configuration file was engaged by opening Notepad to run *AutoDock Vina*. ADT was required to prepare the output .PDBQT file for ligand and to set the grid box's size and center. The grid size dimension and center were $6 \times 8 \times 10$ (x, y, and z) points.

The grid center was designated at x, y, and z dimensions of 14.725, 100.525, and 191.000, respectively, for *C. albicans*, 10 × 8 × 12 (x, y, and z) points, and the grid center was designated at x, y, and z dimensions of -0.04, 22.403, and 19.44 respectively for *C. neoformans*, 8 × 12 × 10 (x, y, and z) points, and the grid center was designated at x, y, and z dimensions of -0.583, 18.748, and 55.246 respectively for *S. typhimurium*, with a grid spacing of 1.000 Å. The prepared file was saved in .PDBQT file format. Ligand-binding affinities were predicted as negative Gibbs free energy (ΔG) scores (kcal/mol), calculated based on the *AutoDock Vina* scoring function. The binding affinity prediction showed how strongly a ligand bound to the receptor. Post-docking analyses were visualized.

RESULTS AND DISCUSSION

In silico Molecular Docking Analysis

In this study, virtual screening was employed to investigate the binding affinities of phytochemicals from *A. indica* to TPPs. Virtual screening, coupled with molecular docking, allows for the efficient evaluation of multiple compounds at once, providing valuable insights into their binding affinities and interactions with target proteins. These findings contribute to understanding the molecular mechanisms underlying the bioactivity of phytochemicals and aid in identifying potential candidates for further experimental validation and drug development. Thus, the binding affinities of 30 bioactive compounds were evaluated and compared.

The molecular docking was carried out between the bioactive compound of *A. indica* and trehalose-6-phosphate phosphatase, which belongs to *C. albicans*, *S. typhimurium*, and *C. neoformans*. The TPPs of these pathogens were selected because their resolution of x-ray crystallography is around 2 Å or less. Higher-resolution crystal structures provide more accurate information about the atomic coordinates of the receptor and its binding sites [10]. This accuracy is crucial for molecular docking studies, as it ensures that the predicted binding poses of ligands are more reliable and closer to the actual binding conformation.

In addition to the phytochemicals, control drugs such as ampicillin, fluconazole, and isoniazid were included in the virtual screening process for comparison. According to Peechakara et al. [11], ampicillin is a widely used antibiotic, while Govindarajan et al., [12] stated that fluconazole is an antifungal medication. On the other hand, isoniazid is an important drug for tuberculosis treatment [13].

These drugs could provide valuable insights into the specificity of the inhibitory effects observed. While these compounds were not originally developed as TPPs inhibitors, they have well-characterized mechanisms of action against different targets. Incorporating these antibiotics as controls allows us to discern whether the effects on TPP activity are due to the inhibition of TPP itself or are secondary consequences of inhibiting other cellular processes targeted by these antibiotics. Thus, it ensures the accuracy and specificity of the findings when evaluating potential TPP inhibitors and their effects on trehalose metabolism.

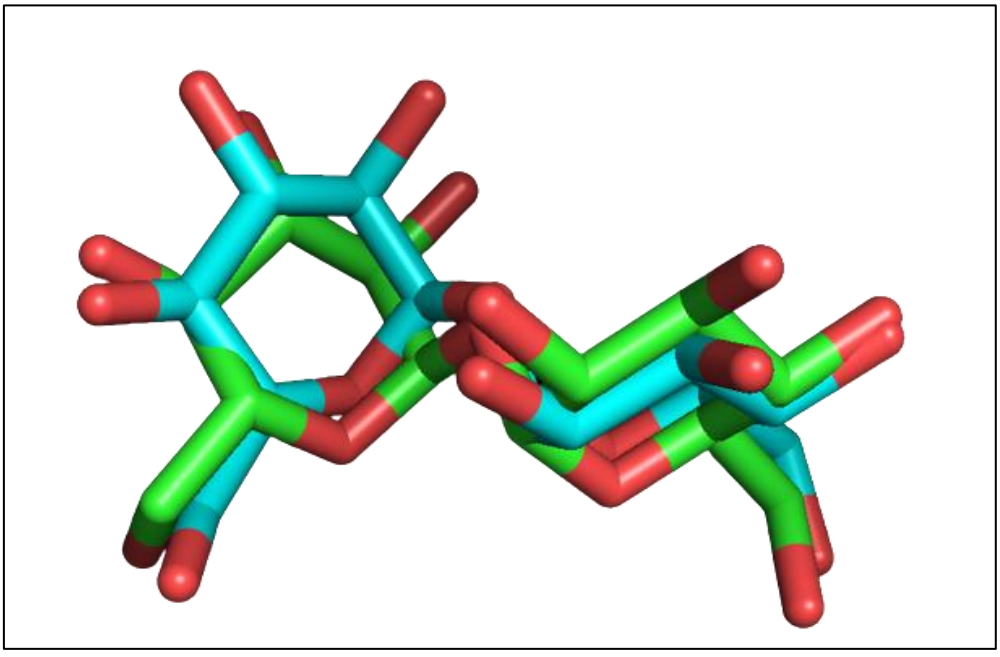

Figure 1. Redocked (cyan) and the crystal structure of trehalose (green).

Docking Validation

The size of the dimensions and the coordinates of the grid box should be validated to ensure that the ligand binding to the binding pocket is in the correct conformation. The validation process is done by docking the original structure of the inhibitor to its sites, also known as the redocking process. Figures 1, 2, and 3 depict the alignment between the original inhibitor (green) and the redocked inhibitor (cyan) in the receptor's binding site. The RMSD values are provided to quantify the deviation between the predicted and crystal conformation of the original inhibitor. The smaller the RMSD values, the smaller the conformation deviation, informing us that the alignment is accurate. The RMSD value ≤ 2 Å is an accepted indicator for accuracy [14].

Table 1. Binding energy between phytochemicals and 5DXI in Autodock Vina.

Bioactive compound	Binding energy (kcal/mol)								
	1	2	3	4	5	6	7	8	9
Trehalose	-8.3	-8.3	-8.2	-8.2	-7.4	-7.3	-7.3	-7.1	-6.4
Ampicillin	-7.2	-6.5	-5.6	-4.4	-	-	-	-	-
Fluconazole	-7.9	-7.8	-7.6	-7.5	-7.5	-7	-7	-6.7	-6.1
Isoniazid	-5.6	-5.5	-5.4	-5.4	-5.4	-5.3	-5.3	-5.2	-5.1
17-hydroxyazadiradione	12.7	-	-	-	-	-	-	-	-
6-desacetylnimbinene	4	4.3	6.2	-	-	-	-	-	-
7-desacetyl-7-benzoylazadiradione	15	-	-	-	-	-	-	-	-
7-desacetyl-7-benzoylgedunin	25.4	27.6	-	-	-	-	-	-	-
Ascorbic acid	-6.3	-6.2	-6.1	-5.9	-5.9	-5.8	-5.7	-5.7	-5.6
Azadiractin K	27.1	27.8	-	-	-	-	-	-	-
Azadiradione	10.5	-	-	-	-	-	-	-	-
Azadirone	26.3	-	-	-	-	-	-	-	-
Beta sitosterol	-1.9	-	-	-	-	-	-	-	-
Catechin	-9	-7.7	-7.5	-	-	-	-	-	-
Gallic acid	-6.4	-6.2	-6.2	-6.2	-6.1	-6	-6	-6	-6
Gedunin	18.9	-	-	-	-	-	-	-	-
Limbocidin	16.3	-	-	-	-	-	-	-	-
Margocin	-7.8	-6.4	-	-	-	-	-	-	-
Margolone	-7.9	-6.6	-5.8	-	-	-	-	-	-
Meliantrol	15.9	-	-	-	-	-	-	-	-
Nimbanal	4.5	-	-	-	-	-	-	-	-
Nimbandiol	1.3	-	-	-	-	-	-	-	-
Nimbidinin	-2.3	-	-	-	-	-	-	-	-
Nimbin	5.6	-	-	-	-	-	-	-	-
Nimbinene	6.7	-	-	-	-	-	-	-	-
Nimbione	-8.7	-7.8	-6.3	-	-	-	-	-	-
Nimbocinone	-7	-7	-6.6	-6.6	-6.6	-6.6	-6.5	-6.4	-6.4
Nimbolide	3.4	-	-	-	-	-	-	-	-
Nimbolin A	42.3	-	-	-	-	-	-	-	-
Nimbolinin	16.8	-	-	-	-	-	-	-	-
Quercetin	-6.8	-5.3	-4.4	-	-	-	-	-	-
Salannin	12.9	-	-	-	-	-	-	-	-
Tiglic acid	-4.7	-4.2	-4.1	-4.1	-4.1	-4	-4	-4	-3.9
Vepinin	26.2	-	-	-	-	-	-	-	-

Molecular Docking Results between Phytochemicals of *A. indica* against *C. albicans* Trehalose-6-phosphate Phosphatase Receptor

Figure 1 shows the results of redocking trehalose (cyan) and the crystal structure of trehalose (green). The superimposition alignment of the original inhibitor (green) and the redocked trehalose crystal conformation (cyan) describes the position of the binding site between the ligand and the receptor with the RMSD values of 0.915 Å. This indicates that the redocking trehalose conformation aligns closely with the original inhibitor's crystal structure, indicating an accurate prediction of the binding site position by redocking.

Binding Affinity Value between Ligands of *A. indica* against *C. albicans* Trehalose-6-phosphate Phosphatase Receptor

Molecular docking between the phytochemicals of *A. indica* and TPPs produced binding affinity, as shown in Table 1. The compound with the highest binding affinity to TPPs is catechin, with an optimal energy of -9.0 kcal/mol. Higher binding affinity indicates a more stable ligand-receptor complex, where the bound state's energy is lower than the unbound state's. The interaction energy between the ligand and receptor is more favorable, resulting in a lower overall binding free energy. This stability suggests that the complex is less likely to dissociate, making it more biologically relevant. Meanwhile, the binding affinity for the control group, ampicillin, fluconazole, and isoniazid, is -7.2 kcal/mol, -7.9 kcal/mol, and -5.6 kcal/mol. The binding affinity of the redocking of trehalose is -8.3 kcal/mol.

Hydrogen, Hydrophobic, and Electrostatic Interaction of the Ligands with *C. albicans* Trehalose-6-phosphate Phosphatase Receptor

During the docking process, several bonding attractions contribute to the interaction energy values, as seen in Table 2. Catechin demonstrated the highest binding affinity to TPPs for *C. albicans* (PDB: 5DXI) with a binding energy of -9.0 kcal/mol. This strong affinity could be attributed to the formation of seven hydrogen bonds and three hydrophobic interactions with 5DXI.

Table 2. Types of binding interaction between the ligands and 5DXI in Autodock Vina.

Ligand	Binding affinity, ΔG (kcal/mol)	Amino acids involved and distance (Å)		
		Hydrogen-Binding Interaction	Hydrophobic Interaction	Electrostatic Interaction
Catechin	-9.0	SER65 (3.02), GLY66 (2.96), ARG142 (2.80), LYS176 (3.34), ASP25 (2.24), ASP231 (2.42), VAL34 (2.12)	HIS140 (5.40), ILE33 (5.11), PRO37 (5.18)	-
Fluconazole	-7.9	ARG67 (3.30), ARG142 (3.05), HIS86 (3.69), GLU180 (3.49)	ILE33 (3.97), ARG67 (4.88)	ASP27 (4.82), ASP27 (4.94), GLU131 (3.56)
Trehalose	-8.3	GLY66 (3.16), ARG67 (3.14), LYS133 (3.23), LYS133 (2.89), ASN178 (2.90), LYS176 (2.99), VAL34 (2.72), GLU131 (3.29), HIS87 (3.35), GLU180 (2.62), ASP27 (3.33), PRO37 (3.54), ARG67 (3.71), HIS140 (3.75), HIS140 (3.72), VAL34 (3.63)	-	-

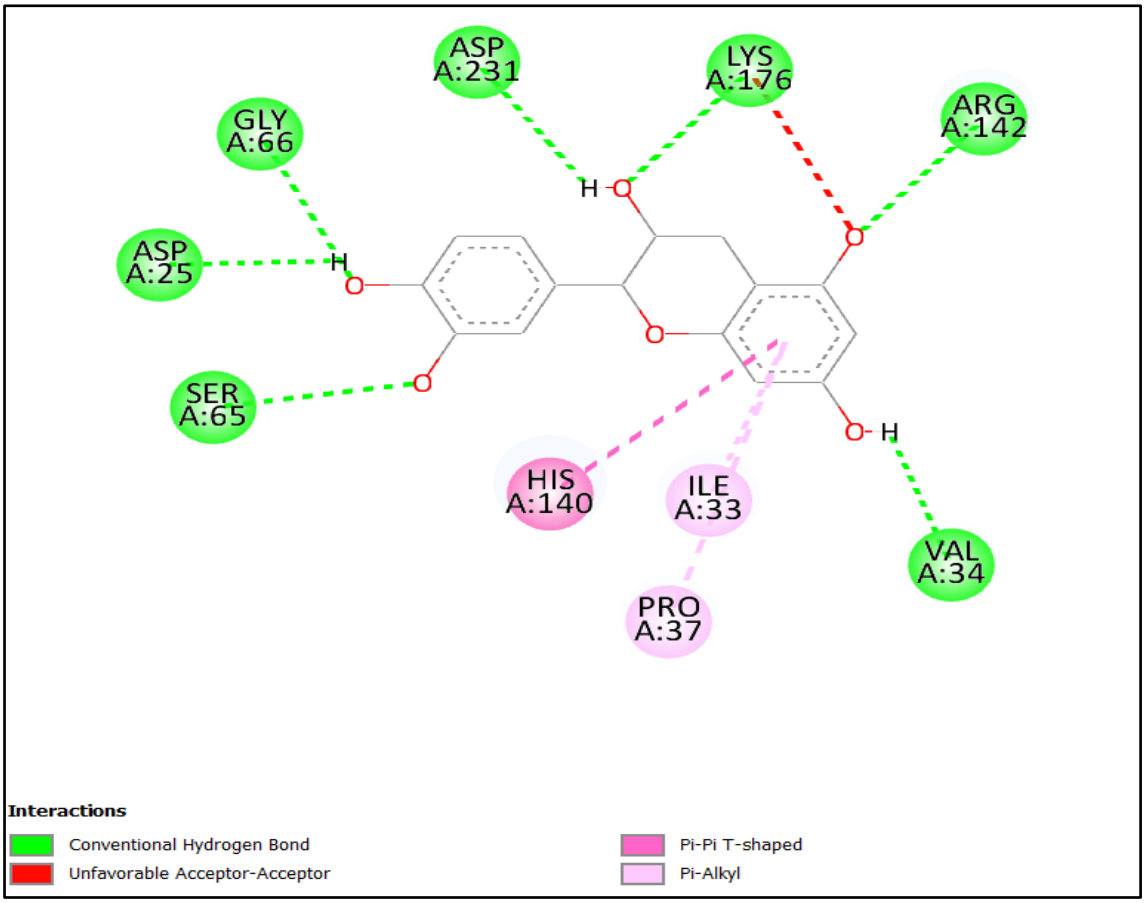

Figure 2. The 2D illustration of the interaction between 5DXI and catechin.

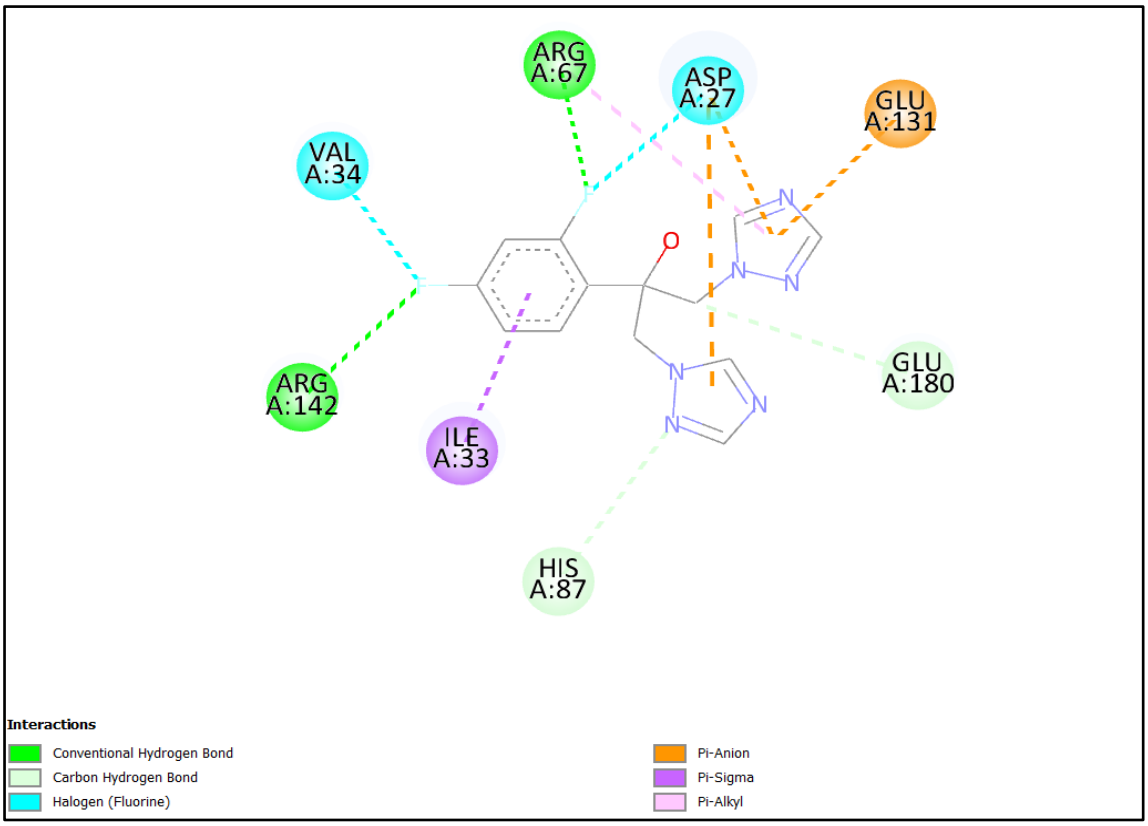

Figure 3. The 2D illustration of the interaction between 5DXI and fluconazole.

Interactions between 5DXI and catechin form a hydrogen bond and hydrophobic interaction, as shown in Figure 2. Catechin forms multiple hydrogen bonds with amino acids in the binding site, which are SER65 (3.02), GLY66 (2.96), ARG142 (2.80), LYS176 (3.34), ASP25 (2.24), ASP231 (2.42), VAL34 (2.12). The amino acids GLY66, ARG142, ASP25, ASP231, and VAL34 have hydrogen bond distances below 3 Å. These hydrogen bonds are short in distance, indicating strong interactions. The presence of multiple strong hydrogen bonds enhances the specificity and stability of the ligand-receptor complex, leading to a higher binding affinity. In addition to hydrogen bonding, catechin also engages in hydrophobic interactions with amino acids like HIS140 (5.40 Å), ILE33 (5.11 Å), and PRO37 (5.18 Å). Although the distances involved in these interactions are longer than hydrogen bonds, they still contribute significantly to binding affinity by maximizing favorable van der Waals interactions. The strong hydrogen bonding and significant hydrophobic interactions further stabilize the ligand-receptor complex, resulting in a higher binding affinity.

Catechin's molecular structure complements the receptor's binding site, allowing it to form favorable interactions. Its arrangement of functional groups and aromatic rings may facilitate optimal interactions with the amino acids in the binding site, enhancing binding affinity.

Fluconazole interacts with 5DXI and forms hydrogen-binding, hydrophobic, and electrostatic interactions, as shown in Figure 3. The hydrogen bonds involve four amino acids: ARG67 (3.30), ARG142 (3.05), HIS86 (3.69), and GLU180 (3.49). Meanwhile, hydrophobic interactions involve two amino acids: ILE33 (3.97) and ARG67 (4.88). The electrostatic interactions involve three amino acids: ASP27 (4.82), ASP27 (4.94), and GLU131 (3.56).

Conversely, Trehalose interacts with 5DXI and forms only hydrogen-binding interactions, as shown in Figure 4. The hydrogen bonds are formed by GLY66 (3.16), ARG67 (3.14), LYS133 (3.23), LYS133 (2.89), ASN178 (2.90), LYS176 (2.99), VAL34 (2.72), GLU131 (3.29), HIS87 (3.35), GLU180 (2.62), ASP27 (3.33), PRO37 (3.54), ARG67 (3.71), HIS140 (3.75), HIS140 (3.72) and VAL34 (3.63) which is 16 bonds in total. No electrostatic and hydrophobic interactions can be observed between 5DXI and trehalose.

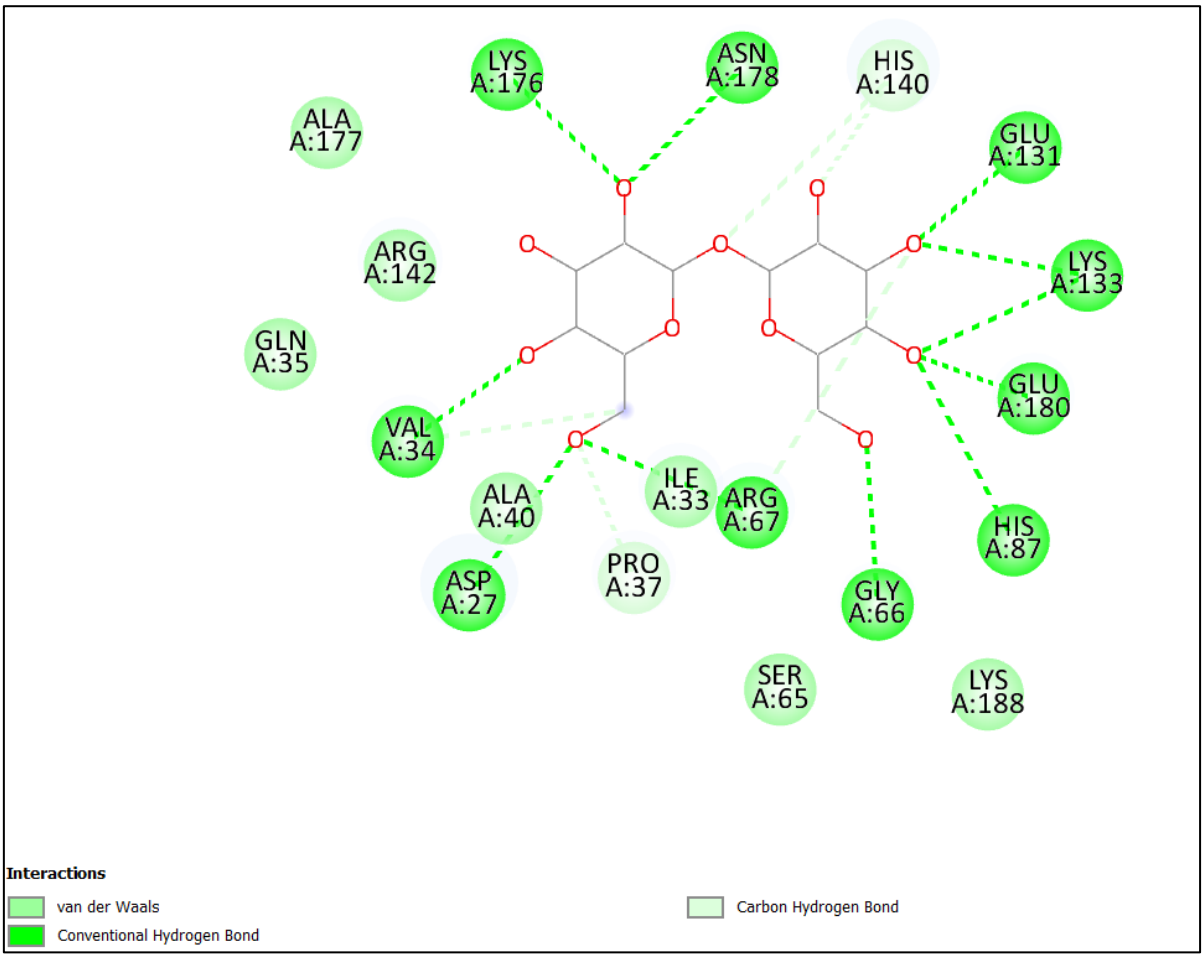

Figure 4. The 2D illustration of the interaction between 5DXI and trehalose.

Thus, catechin exhibits the highest binding affinity among the provided ligands due to its ability to form multiple strong hydrogen bonds and significant hydrophobic interactions with the receptor. These interactions contribute to the ligand-receptor complex's specificity, stability, and overall structural compatibility, resulting in a higher binding affinity for catechin than fluconazole and trehalose.

Molecular Docking Results between Phytochemicals of *A. indica* against *C. neoformans* Trehalose-6-phosphate Phosphatase Receptor

Figure 5 shows the results of redocking trehalose (cyan) and the crystal structure of trehalose (green). The superimposition alignment matches the original inhibitor (green), and the trehalose crystal conformation (cyan) describes the position of the binding site between the ligand and the receptor with the RMSD values of 1.384 Å. This indicates a higher deviation between the redocked trehalose-6-phosphate, and the crystal structure compared to Figure 1. The alignment still demonstrates some agreement between the original inhibitor and the redocked pose but with a slightly increased deviation in positioning.

Binding Affinity Value between Ligands of *A. indica* against *C. neoformans* Trehalose-6-phosphate Phosphatase Receptor

Molecular docking between the phytochemicals of *A. indica* and TPPs produced binding affinity, as shown in Table 3. The compound with the highest binding affinity to TPPs is margocin, with an optimal energy of -9.9 kcal/mol, followed by catechin with -9.7 kcal/mol. Meanwhile, the binding affinity for the control group, ampicillin, fluconazole, and isoniazid, is -8.8 kcal/mol, -8.3 kcal/mol, and -6.3 kcal/mol. The binding affinity of the redocking of trehalose-6-phosphate is -10.4 kcal/mol.

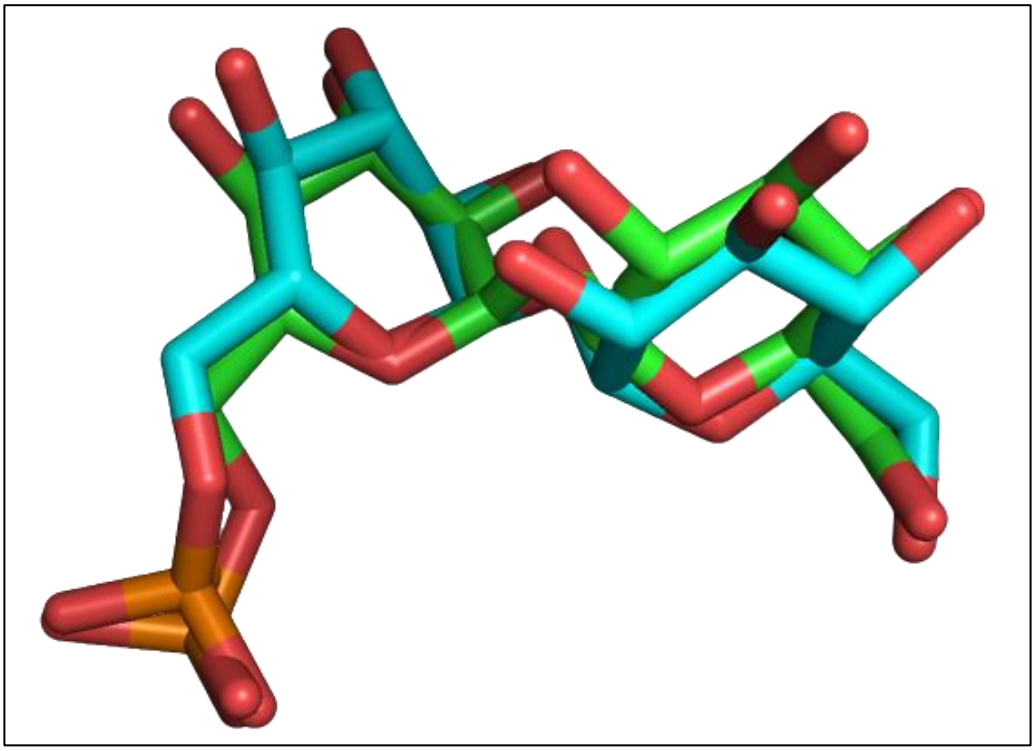

Figure 5. Redocked (cyan) and the crystal structure of trehalose (green).

Table 3. Binding energy between phytochemicals and 5DX9 in ADT Vina.

Bioactive compound	Binding energy (kcal/mol)								
	1	2	3	4	5	6	7	8	9
Trehalose	-10.4	-9.4	-9.4	-9.3	-9.1	-8.5	-8.4	-8.4	-8.2
Ampicillin	-8.8	-7.8	-7.7	-7.6	-7.1	-6.9	-6.8	-6.8	-6.7
Fluconazole	-8.3	-8.3	-8.1	-8.1	-8	-7.9	-7.9	-7.7	7.6
Isoniazid	-6.3	-6.3	-6.1	-5.8	-5.6	-5.5	-5.5	-5.4	-5.4
17 hydroxyazadiradione	0.1	0.4	-	-	-	-	-	-	-

6 desacetylnimbinene	-5.7	-5.5	-5.1	-4.8	-2.8	-	-	-	-
7 desacetyl 7 benzoylazadiradione	5.4	6.6	8.3	-	-	-	-	-	-
7 desacetyl 7 benzoylgedunin	4.1	5.2	6.1	-	-	-	-	-	-
Ascorbic acid	-7.1	-6.9	-6.7	-6.7	-6.6	-6.5	-6.5	-6.4	-6.4
Azadiractin K	6.5	6.7	7.5	9	-	-	-	-	-
Azadiradione	0.7	0.8	2		-	-	-	-	-
Azadirone	-0.6	1.5	-	-	-	-	-	-	-
Beta sitosterol	-5.6	-	-	-	-	-	-	-	-
Catechin	-9.7	-9.2	-8.9	-8.5	-8.3	-8.3	-8.1	-7.1	-
Gallic acid	-7.3	-7.2	-7.1	-7.1	-7	-7	-6.9	-6.9	-6.8
Gedunin	-1.4	-	-	-	-	-	-	-	-
Limbocidin	10	-	-	-	-	-	-	-	-
Margocin	-9.9	-7.6	-7.2	-	-	-	-	-	-
Margolone	-8.5	-7.5	-7.5	-7.3	-7.2	-6.4	-	-	-
Meliantrol	-3.8	-	-	-	-	-	-	-	-
Nimbanal	-4.8	-3.3	-3.1	-2.2	-	-	-	-	-
Nimbandiol	-5.8	-5.2	-	-	-	-	-	-	-
Nimbidinin	-5.9	-5.3	-	-	-	-	-	-	-
Nimbin	-4.9	-4.7	-	-	-	-	-	-	-
Nimbinene	-4.7	-2.9	-2.7	-	-	-	-	-	-
Nimbione	-8.8	-8.4	-8.3	-8	-7	-6.8	-6.8	-6.4	-
Nimbocinone	-7.5	-7.3	-7.1	-7.1	-6.9	-6.8	-6.7	-6.5	-6.5
Nimbolide	-5.2	-3	-	-	-	-	-	-	-
Nimbolin A	12.9	-	-	-	-	-	-	-	-
Nimbolinin	10.4	-	-	-	-	-	-	-	-
Quercetin	-9.2	-9	-8.9	-8.8	-8.8	-8.5	-7.9	-7.8	-7.7
Salannin	0.3	2.1	2.4	-	-	-	-	-	-
Tiglic acid	-4.9	-4.9	-4.7	-4.6	-4.3	-4.3	-4.2	-4.2	-4.2
Vepinin	0.1	-	-	-	-	-	-	-	-

Table 4. Types of binding interaction between the ligands and 5DX9 in Autodock Vina.

Ligand	Binding affinity, ΔG (kcal/mol)	Amino acids involved and distance (Å)		
		Hydrogen-Binding Interaction	Hydrophobic Interaction	Electrostatic Interaction
Margocin	-9.9	ASN24 (2.97 Å), GLY65 (3.12 Å), LYS188 (3.08 Å)	VAL33 (4.84 Å)	ASP26 (4.10 Å)
Catechin	-9.7	GLY65 (2.89 Å), ARG142 (2.86 Å), ARG142 (2.98 Å), LYS176 (3.32 Å), ASP214 (2.99 Å), LYS176 (2.36 Å)	ASP26 (3.76 Å), ILE32 (4.69 Å)	ASP26 (3.87 Å)
Ampicillin	-8.8	ARG142 (3.29 Å), LYS188 (3.16 Å), ASP26 (3.60 Å), VAL33 (3.96 Å)	ILE32 (4.56 Å), VAL33 (5.44 Å), PRO36 (5.34 Å), ALA39 (4.98 Å)	ARG66 (4.30 Å)

Trehalose-6-phosphate	-10.4	ASN24 (3.11 Å), VAL33 (3.08 Å), GLY65 (2.87 Å), THR138 (3.15 Å), ASN178 (2.99 Å), LYS188 (2.80 Å), GLU131(2.26 Å), GLU180(2.58 Å), ASP26(2.63 Å), SER64(1.84 Å), VAL33(1.84 Å), VAL33(3.49 Å)	ILE32 (4.93 Å)	ASP26(3.70 Å)

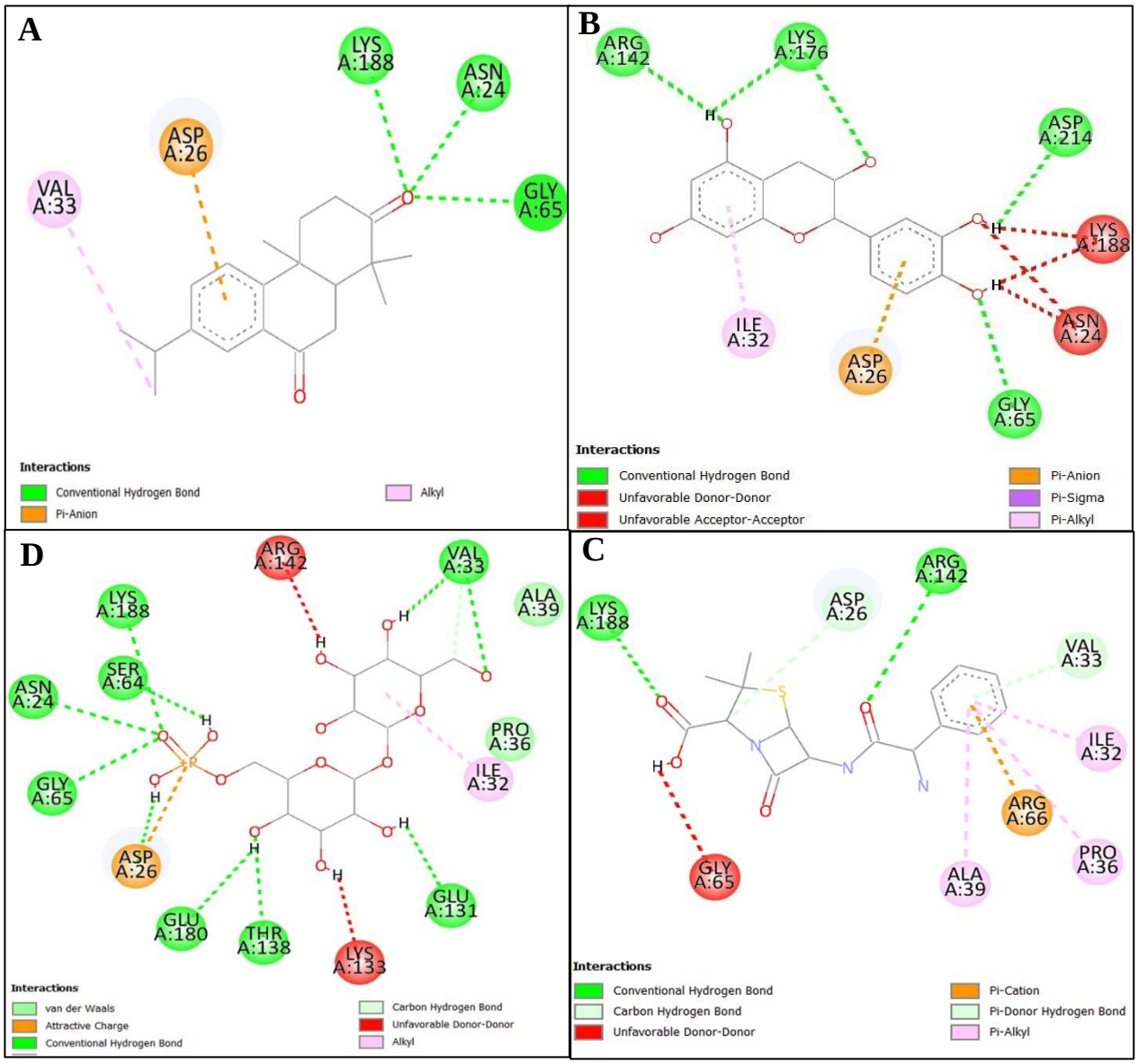

Figure 6. The 2D illustration of interaction (A) margocin, (B) catechin, (C) ampicillin, and (D) Trehalose-6-phosphate toward 5DX9.

Hydrogen, Hydrophobic, and Electrostatic Interaction of the Ligands toward *C. neoformans* Trehalose-6-phosphate Phosphatase Receptor

Due to their close binding affinity values and high affinities compared to other compounds, margocin and catechin, have been subjected to detailed analysis regarding the amino acid residues involved in bond formation, the types of bonds, and the bond distances (Table 4).

Margocin interacts with ASN24, GLY65, and LYS188 through hydrogen bonds, with bond distances ranging from 2.97 Å to 3.12 Å. Similarly,

catechin forms hydrogen bonds with GLY65, ARG142, LYS176, and ASP214, with bond distances ranging from 2.86 Å to 3.32 Å. These interactions contribute significantly to their binding affinities. Margocin engages in a hydrophobic interaction with VAL33 at 4.84 Å, while Catechin interacts with ILE32 at 4.69 Å. These hydrophobic interactions also contribute to the overall stability of the ligand-receptor complexes. Margocin forms an electrostatic interaction with ASP26 at 4.10 Å, while catechin interacts with ASP26 at 3.76 Å and 3.87 Å. These electrostatic interactions contribute to stabilizing the complexes, though to a lesser extent than hydrogen bonds and hydrophobic interactions.

Conversely, trehalose-6-phosphate interacts with 5DX9 and forms three types of interaction, such as the previously mentioned two ligands (Figure 6-D). Trehalose-6-phosphate forms hydrogen bonds with multiple amino acids, including ASN24, VAL33, GLY65, THR138, ASN178, and LYS188, with bond distances ranging from 1.84 Å to 3.49 Å. These strong hydrogen bonds play a crucial role in its high binding affinity. Trehalose-6-phosphate engages in a hydrophobic interaction with ILE32 at 4.93 Å, contributing to its overall stability within the binding site. Trehalose-6-phosphate forms an electrostatic interaction with ASP26 at 3.70 Å, further stabilizing the ligand-receptor complex.

Overall, the high binding affinities of Margocin, Catechin, and Trehalose-6-phosphate can be attributed to their strong interactions with key amino acid residues in the binding site, including hydrogen bonds, hydrophobic interactions, and electrostatic interactions. While Margocin and Catechin exhibit slightly lower binding affinities than Trehalose-6-phosphate, they still demonstrate significant binding strengths, primarily due to their extensive hydrogen-bonding networks and additional hydrophobic interactions.

Molecular Docking Results between Phytochemicals of *A. indica* against *S. typhimurium* Trehalose-6-phosphate Phosphatase Receptor

Figure 7 exhibits a lower RMSD value of 0.583 Å, the lowest RMSD value among the others. This suggests that the redocked trehalose and the crystal structure possess remarkably similar conformation, implying a better prediction of the ligand-receptor interaction.

Binding Affinity Value between Phytochemicals of *A. indica* against *S. typhimurium* Trehalose-6-phosphate Phosphatase Receptor

Molecular docking between the phytochemicals of *A. indica* and TPPs produced binding affinity, as shown in Table 5. The compound with the highest binding affinity to TPPs is catechin, with an optimal energy of -9.0 kcal/mol. Meanwhile, the binding affinity for the control group, ampicillin, fluconazole, and isoniazid, is -7.6 kcal/mol, -7.8 kcal/mol, and -6.0 kcal/mol. The binding affinity of the redocking of trehalose is -8.7 kcal/mol.

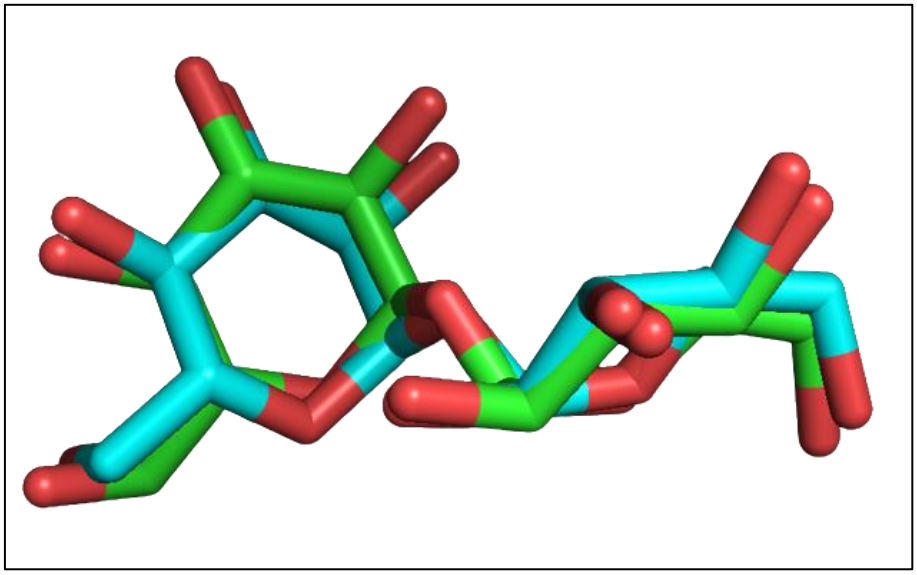

Figure 7. Redocked (cyan) and the crystal structure of trehalose (green).

Table 5. Binding energy between phytochemicals and modelled 6UPD in ADT Vina.

Ligand	Binding energy (kcal/mol)								
	1	2	3	4	5	6	7	8	9
Trehalose	-8.7	-8.6	-7.8	-7.6	-7.5	-7.5	-7.4	-7.4	-7
Ampicillin	-7.6	-7.5	-7.5	-7.1	-6.4	-5.9	-5.6	-5.5	-
Fluconazole	-7.8	-7.7	-7.6	-7.5	-7.5	-7.4	-7.4	-7.3	-7.3
Isoniazid	-6	-5.5	-5.5	-5.3	-5.3	-5.2	-5.1	-5	-5
17 hydroxyazadiradione	-2.6	-1.5	-	-	-	-	-	-	-
6 desacetylnimbinene	-7.1	-	-	-	-	-	-	-	-
7 desacetyl 7 benzoylazadiradione	-3.7	-0.9	-	-	-	-	-	-	-
7 desacetyl 7 benzoylgedunin	-4.3	-	-	-	-	-	-	-	-
Ascorbic acid	-6.1	-5.8	-5.8	-5.7	-5.6	-5.4	-5.4	-5.3	-5.3
Azadiractin K	7.8	-	-	-	-	-	-	-	-
Azadiradione	-4	-	-	-	-	-	-	-	-
Azadirone	-5.4	-3.1	-3	-	-	-	-	-	-
Beta sitosterol	-4.6	-	-	-	-	-	-	-	-
Catechin	-9	-9	-8.7	-8.6	-8.6	-8.2	-8.2	-7.4	-7.1
Gallic acid	-6.2	-6.2	-6.2	-6.2	-6.1	-6.1	-6.1	-6	-5.9
Gedunin	-5	-	-	-	-	-	-	-	-
Limbocidin	7	-	-	-	-	-	-	-	-
Margocin	-7.8	-7.8	-7.7	-7.4	-6.7	-6.6	-5.9	-5.6	-
Margolone	-7.8	-7.6	-6.9	-6.8	-6.8	-6.6	-5.9	-5.1	-4.9
Meliantrol	-0.9	9	1.8	-	-	-	-	-	-
Nimbanal	0.3	1	1.8	-	-	-	-	-	-
Nimbandiol	-2.5	-1	-0.1	-	-	-	-	-	-
Nimbidinin	-6.1	-3.5	-	-	-	-	-	-	-
Nimbin	-6.3	-	-	-	-	-	-	-	-
Nimbinene	1.1	2.7	3.5	-	-	-	-	-	-
Nimbione	-8.9	-8	-7.9	-7.6	-7.6	-6.9	-6.9	-6.8	-6.5
Nimbocinone	-6.3	-6.2	-6	-6	-5.9	-5.9	-5.9	-5.9	-5.9
Nimbolide	-2.7	-1	-	-	-	-	-	-	-
Nimbolin A	0.5	-	-	-	-	-	-	-	-
Nimbolinin	11	-	-	-	-	-	-	-	-
Quercetin	-8.8	-8.7	-8.4	-8.3	-7.9	-7.8	-7.7	-7.5	-7.3
Salannin	1.6	3.9	-	-	-	-	-	-	-
Tiglic acid	-4.4	-4.3	-4.3	-4.1	-4	-4	-3.9	-3.9	-3.9
Vepinin	0.2	1.8	-	-	-	-	-	-	-

Hydrogen, Hydrophobic, and Electrostatic Interaction of the Ligands with Trehalose-6-phosphate Phosphatase of *S. typhimurium* Receptor

Catechin demonstrated the highest binding affinity *S. Typhimurium* (PDB: 6UPD), with a binding energy of -9.0 kcal/mol. This strong affinity could be attributed to forming two hydrogen bonds, two hydrophobic interactions, and one electrostatic interaction, as shown in Table 6.

Catechin exhibits interactions with 6UPD involving hydrogen-binding and hydrophobic interactions (Figure 8). The hydrogen-binding interactions of catechin include two bonds, which are ARG13 (3.31 Å) and LYS163 (2.11 Å). The hydrogen bond distance with LYS163 is notably short, indicating a strong interaction, which contributes significantly to the high binding affinity observed. Catechin engages in hydrophobic interactions with VAL165 (3.94 Å) and PRO32 (4.62 Å), indicating interactions with

nonpolar amino acids in the receptor binding site. Catechin forms an electrostatic interaction with ARG134 (4.22 Å), further stabilizing the ligand-receptor complex.

Fluconazole interacts with 5DXI and forms hydrogen-binding, hydrophobic, and electrostatic interactions, as shown in Figure 3. The hydrogen bonds involve four amino acids: ARG67 (3.30), ARG142 (3.05), HIS86 (3.69), and GLU180 (3.49). Meanwhile, hydrophobic interactions involve two amino acids: ILE33 (3.97) and ARG67 (4.88). The electrostatic interactions involve three amino acids: ASP27 (4.82), ASP27 (4.94), and GLU131 (3.56).

Table 6. Types of binding interaction between ligands and 6UPD in Autodock Vina.

Ligand	Binding affinity, ΔG (kcal/mol)	Amino acids involved and distance (Å)		
		Hydrogen-Binding Interaction	Hydrophobic Interaction	Electrostatic Interaction
Catechin	-9.0	ARG13 (3.31 Å), LYS163 (2.11 Å)	VAL165 (3.94 Å), PRO32 (4.62 Å)	ARG134 (4.22 Å)
Fluconazole	-7.8	LYS29 (3.11 Å), GLU123 (3.67 Å)	HIS132 (4.62 Å), ILE28 (5.21 Å), PRO32 (5.02 Å), ALA130 (4.71 Å), VAL165 (4.60 Å)	ASP22:OD1 (4.12 Å), ASP199:OD2 (3.76 Å)
Trehalose	-8.8	LYS29 (2.96 Å), LYS125 (2.85 Å), ARG134 (3.02 Å), ARG134 (3.17 Å), LYS163 (3.33 Å), GLU123 (3.21 Å), GLU167 (3.17 Å), GLY61 (3.64 Å)	-	-

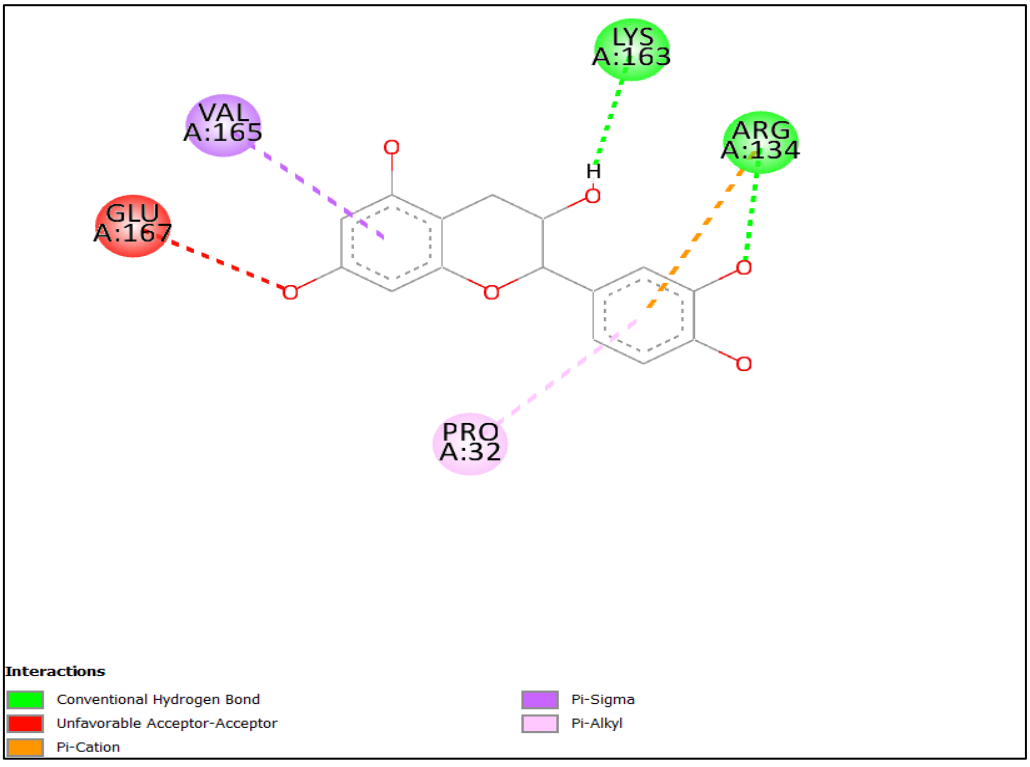

Figure 8. The 2D illustration of the interaction between 6UPD and catechin.

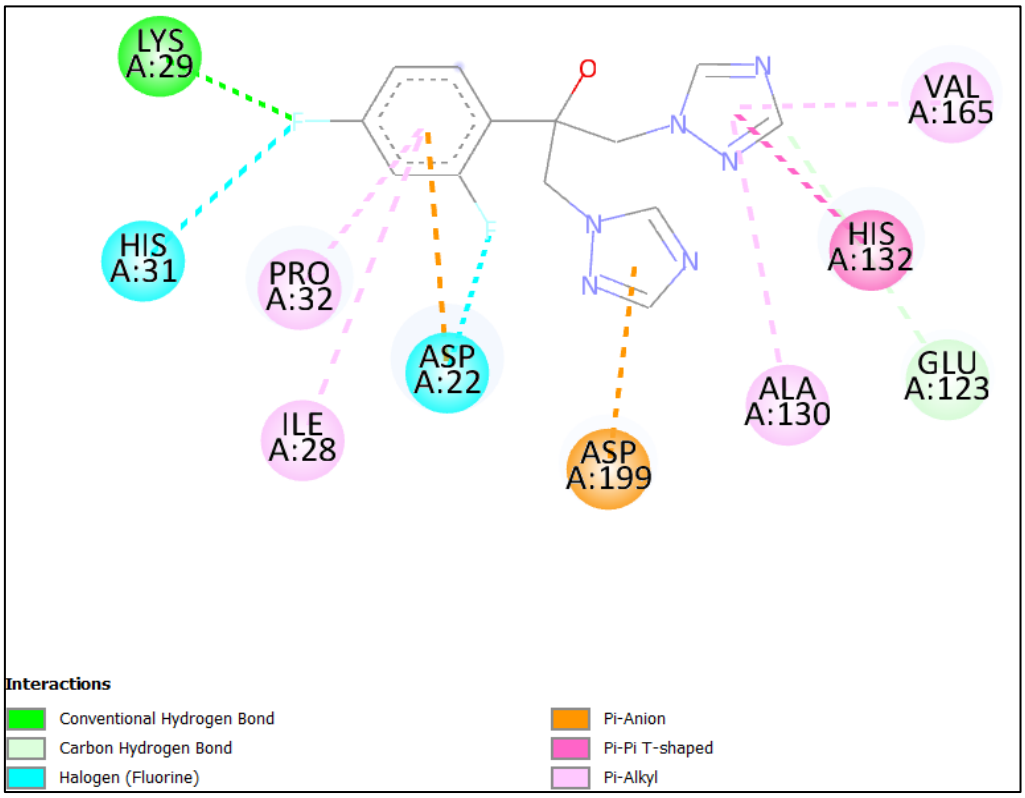

Figure 9. The 2D illustration of the interaction between 6UPD and fluconazole.

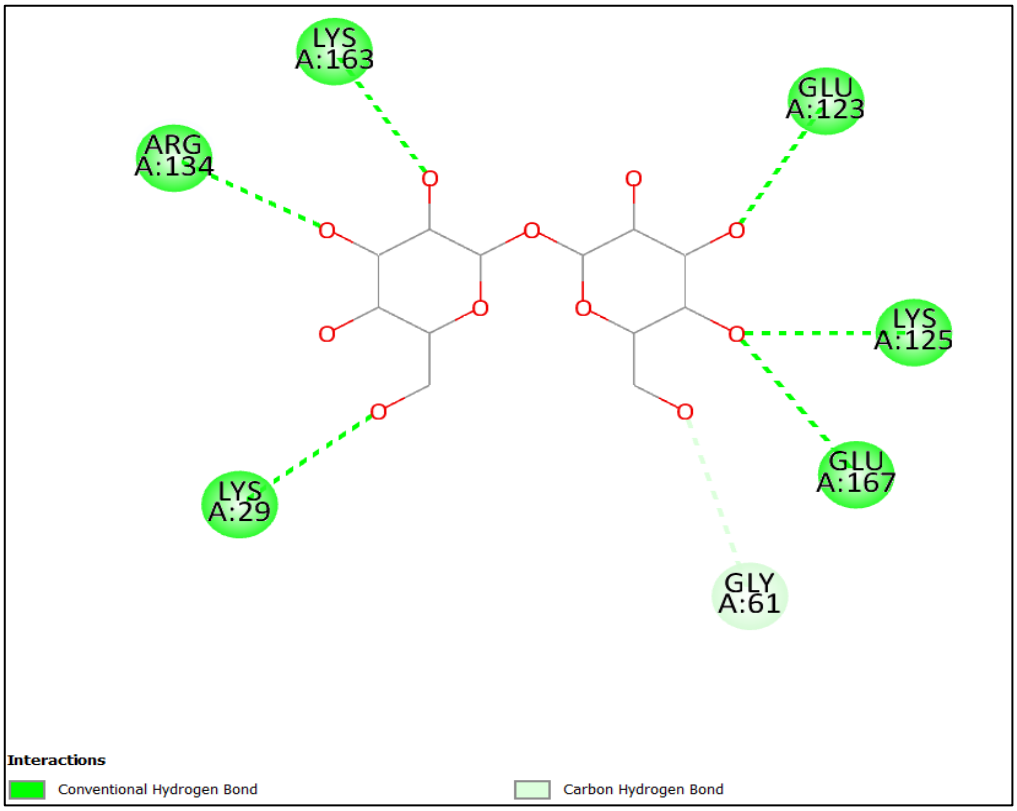

Figure 10. The 2D illustration of the interaction between 6UPD and trehalose.

Trehalose interacts with 6UPD through hydrogen-binding interactions, while no hydrophobic or electrostatic interactions are observed (Figure 12). The hydrogen bonds of trehalose involve seven amino acids which are LYS29 (2.96 Å), LYS125 (2.85 Å), ARG134 (3.02 Å), ARG134 (3.17 Å), LYS163 (3.33

Å), GLU123 (3.21 Å), GLU167 (3.17 Å), and GLY61 (3.64 Å). The highest binding affinity recorded for the controls and each TPPs is -7.2 kcal/mol, -8.8 kcal/mol, and -7.8 kcal/mol for fluconazole, ampicillin, and fluconazole, respectively. The results indicated that a few phytochemicals from *A. indica* showed comparable or better binding affinities to the control drugs, highlighting their potential as alternative or complementary therapeutic agents.

Catechin emerges as a potential common binding ligand for all three trehalose-6-phosphate-phosphatase (TPPs) due to its high binding affinity observed across all three. Additionally, margocin exhibits the highest binding affinity against *C. neoformans* trehalose-6-phosphate phosphatase receptor, highlighting its potential as a significant ligand.

CONCLUSION

This study has identified catechin as a promising inhibitor of trehalose-6-phosphate-phosphatase (TPPs) of *C. albicans*, *C. neoformans*, and *S. Typhimurium* through molecular docking analysis. Catechin exhibited better binding energies than the redocked native ligands and the control drugs, except for the binding energy against TPPs of *C. neoformans*. However, further *in vitro* and *in vivo* experiments are required to validate the efficacy and safety of these in silico results.

ACKNOWLEDGEMENTS

The authors received no financial support for the research.

REFERENCES

1. Qiu, L., Wei, X. Y., Wang, S. J. and Wang, J. J. (2020). Characterization of trehalose-6-phosphate phosphatase in trehalose biosynthesis, asexual development, stress resistance and virulence of an insect mycopathogen. *Pesticide Biochemistry and Physiology*, **163**, 185–192.

2. Kim, J. H., Kim, J. W., Jo, J., Straub, J. H., Cross, M., Hofmann, A. & Kim, J. S. (2021). Characterization of trehalose-6-phosphate phosphatases from bacterial pathogens. *Biochimica et Biophysica Acta (BBA) - Proteins and Proteomics*, **1869**, 140564.

3. Tang, B., Wang, S., Wang, S. G., Wang, H. J., Zhang, J. Y. and Cui, S. Y. (2018). Invertebrate Trehalose-6-Phosphate Synthase Gene: Genetic Architecture, Biochemistry, Physiological Function, and Potential Applications. *Frontiers in Physiology*, **9**, 30.

4. Suthisawat, S., Gourlay, L. J., Bolognesi, M., Boonyuen, U. and Vanaporn, M. (2020) Functional and structural analysis of trehalose-6-phosphate phosphatase from Burkholderia pseudomallei: Insights into the catalytic mechanism. *Biochemical and Biophysical Research Communications*, **523**, 979–984.

5. Islas, J. F., Acosta, E., G-Buentello, Z., Delgado-Gallegos, J. L., Moreno-Treviño, M. G., Escalante, B. and Moreno-Cuevas, J. E. (2020) An overview of Neem (*Azadirachta indica*) and its potential impact on health. *Journal of Functional Foods*, 74.

6. Torres, P. H. M., Sodero, A. C. R., Jofily, P. and Silva-Jr, F. P. (2019) Key Topics in Molecular Docking for Drug Design. *International Journal of Molecular Sciences*, **20**, 18.

7. Abdullah, M. Z., Bakar, L. M., Arief Ichwan, S. J., Othman, N. and Taher, M. (2022) Molecular docking study of naturally derived β-mangostin with antiapoptotic Bcl-2 proteins toward oral cancer treatment. *ESTEEM Academic Journal*, **18**, 128–138.

8. Umesh, H. R., Ramesh, K. V. and Devaraju, K. S. (2020) Molecular docking studies of phytochemicals against trehalose–6–phosphate phosphatases of pathogenic microbes. *Beni-Suef University Journal of Basic and Applied Sciences*, **9**, 1.

9. Trott, O. and Olson, A. J. (2009) AutoDock Vina: Improving the speed and accuracy of docking with a new scoring function, efficient optimization, and multithreading. *Journal of Computational Chemistry*, **31**, 2.

10. Liebeschuetz, J. W. (2021). The Good, the Bad, and the Twisted Revisited: An Analysis of Ligand Geometry in Highly Resolved Protein–Ligand X-ray Structures. *Journal of Medicinal Chemistry*, **64(11)**, 7533–7543.

11. Peechakara, B. V., Basit, H. and Gupta, M. (2022) Ampicillin. *PubMed*; StatPearls Publishing.

12. Govindarajan, A., Bistas, K. G. and Aboeed, A. (2020) Fluconazole. *PubMed*; StatPearls Publishing.

13. O'Connor, C. and Brady, M. F. (2023) Isoniazid. *PubMed*; *StatPearls Publishing*.

14. Ideris, S., Imran, S., Abd Latip, N. and Osman, C. P. (2024) Goniothalamin and Its Analogues as Potential Inhibitors of Plasmodium falciparum Lactate Dehydrogenase Enzyme: Molecular Docking, Molecular Dynamics Simulation Studies, and Pharmacokinetics Analysis. *Malaysian Journal of Chemistry*, **26(1)**, 27–39